

# Proceedings of the Institution of Mechanical Engineers, Part G: Journal of Aerospace Engineering

<http://pig.sagepub.com/>

---

## **A multilevel framework for optimization of an aircraft wing incorporating postbuckling effects**

S Qu, D Kennedy and C A Featherston

*Proceedings of the Institution of Mechanical Engineers, Part G: Journal of Aerospace Engineering* published online 9

November 2011

DOI: 10.1177/0954410011415158

The online version of this article can be found at:

<http://pig.sagepub.com/content/early/2011/11/08/0954410011415158>

---

Published by:



<http://www.sagepublications.com>

On behalf of:



[Institution of Mechanical Engineers](http://www.imechE.org)

**Additional services and information for *Proceedings of the Institution of Mechanical Engineers, Part G: Journal of Aerospace Engineering* can be found at:**

**Email Alerts:** <http://pig.sagepub.com/cgi/alerts>

**Subscriptions:** <http://pig.sagepub.com/subscriptions>

**Reprints:** <http://www.sagepub.com/journalsReprints.nav>

**Permissions:** <http://www.sagepub.com/journalsPermissions.nav>

>> [OnlineFirst Version of Record](#) - Nov 9, 2011

[What is This?](#)

# A multilevel framework for optimization of an aircraft wing incorporating postbuckling effects

S Qu, D Kennedy, and C A Featherston\*

Cardiff School of Engineering, Cardiff University, Cardiff, UK

*The manuscript was received on 31 August 2010 and was accepted after revision for publication on 7 June 2011.*

DOI: 10.1177/0954410011415158

**Abstract:** The optimization of aerospace structures is a very complex problem, owing to the hundreds of design variables a multidisciplinary optimization may contain, so that multilevel optimization is required. This paper presents recent developments to the optimization software VICONOPT MLO, a multilevel optimization interface between the analysis and design software packages VICONOPT and MSC/NASTRAN. The software developed, VICONOPT MLOP (Multilevel Optimization with Postbuckling) incorporates postbuckling behaviour, allowing individual panels to buckle before the design load is reached, while carrying load at a reduced stiffness. By combining two iterative cycles the first of which (known as the analysis cycle) calculates these reduced postbuckling stiffnesses at an individual panel level in order to converge on an appropriate load distribution at a whole structure or system level and the second of which (known as the design cycle) optimizes individual panels based on this load redistribution to converge on an optimized mass for the whole structure. The paper provides a detailed overview of the functionality of the software and a case study is conducted into the optimization of a composite aircraft wing. The results of the case study show substantial mass savings, proving the software's capabilities when dealing with such problems. The time taken for this multilevel optimization also demonstrates the efficiency of the software.

**Keywords:** exact strip, finite element analysis, optimization, postbuckling, composite

## 1 INTRODUCTION

One of the most important objectives of aircraft structural design is minimizing weight. Therefore, modern design increasingly utilizes high-performance materials, such as carbon-fibre reinforced composites. When combined with efficient analysis and optimization tools, these can lead to significantly increased stiffness, strength, and reliability, while reducing the weight of structural components and systems.

Structural optimization can be defined as the rational finding of a structural design that is the best of all possible designs for a chosen objective and a given set of geometrical and behavioural constraints [1].

Various optimization methods have evolved over the years, some of which are better suited to structural engineering applications than others. Numerous methods have been developed to solve constrained optimization problems, which engineering optimization problems almost always are. Generally, these methods can be categorized as indirect and direct. Indirect methods convert the constrained optimization problem into an equivalent unconstrained problem, while direct methods attempt to solve the constrained optimization problem as it is. Examples of indirect methods include penalty-function methods and augmented Lagrange multiplier methods [2–4]. Direct methods include the method of feasible directions, dual methods, and reduced gradient methods [5].

The exact strip software VICONOPT [6, 7] is based on the Wittrick–Williams algorithm [8, 9] and provides

\*Corresponding author: Cardiff School of Engineering, Cardiff University, Queen's Buildings, The Parade, Cardiff CF24 3AA, UK. email: FeatherstonCA@cardiff.ac.uk

a powerful tool for preliminary aircraft design, which performs initial buckling, postbuckling and free vibration analyses of prismatic assemblies of isotropic and anisotropic plates. It covers any prismatic assembly of anisotropic plates which can carry any combination of longitudinally invariant in-plane stresses.

In the simplest (VIPASA) form of the analysis [10], the buckling or vibration mode is assumed to vary sinusoidally in the prismatic direction. This approach gives exact solutions for isotropic and orthotropic panels with simply supported ends carrying no shear load, but otherwise the results are conservative, especially for overall buckling. The main advantage of VIPASA over finite strip and finite element methods is its speed. When compared to the finite element program STAGS (Structural Analysis of General Shells) [11], VIPASA has proved to be 1000 times faster when finding the eigenvalues of a panel [12]. Improved solutions are obtained using VICON analysis [13], which finds the shear modes for an infinitely long structure by coupling sinusoidal responses using a Lagrangian multiplier approach to satisfy the end conditions. Compared with the finite element program STAGS, VICON has proved to be 150 times quicker [12].

In a VICONOPT design problem, a range of different design variables (e.g. plate widths and ply thicknesses) are optimized subject to buckling, strength, stiffness, and geometric constraints, in order to obtain the minimum mass. However, in the context of a more complex structure, such as an aircraft wing, it is important to note that design changes to individual panels influence the stress distribution over the whole structure, and must also be compatible with the geometry of adjacent panels.

The potential to make the optimization of complex structures more manageable by applying a multilevel approach, has encouraged an increase in research activity over recent years, with the majority of work being carried out in the United States. In 1990 the Group for Aeronautical Research and Technology in Europe (GARTEUR) set up an Action Group to review the progress made in the European aerospace community with applying optimization techniques to aircraft wing design as a multilevel problem. The GARTEUR Action Group recommended the development of multilevel optimization software in order to automate many of the procedures explored. In this way, the complexities affecting the optimization process could be better investigated. A summary of the work, results and recommendations of the GARTEUR Action Group has been published in a three volume report, parts of which is available in the open literature [14–16].

More recently new computational procedures for optimization [17] and metamodelling methodology [18] have been developed, in order both to give more accurate results and also to incorporate time efficiencies for complex structural optimization problems. Additionally, researchers are looking for insight based initially on small models e.g. plates or panels, to investigate multi-objective optimization procedures [19, 20].

## 2 POSTBUCKLING ANALYSIS

There is increasing pressure to extend the design envelope into the postbuckling region where this is stable, resulting in more efficient structures limited only by material failure criterion. GARTEUR published a technical report AG-25 [21] on buckling, postbuckling, and collapse research work on aerospace structures and gave recommendations based on three benchmark tests carried out by Airbus France, SAAB and DLR separately. The POSICOSS (Improved POSTbuckling SIMulation for Design of Fibre COMposite Stiffened Fuselage Structures) project was carried out based on the GARTEUR recommendations and aimed to provide an improved, fast and reliable approach for postbuckling analysis and design of fibre composite stiffened panels and design guidelines based on experimental data [22]. This was followed by the COCOMAT (Improved MATERIAL Exploitation at Safe Design of COMposite Airframe Structures by Accurate Simulation of COLLAPSE) project which looked specifically at simulating future design scenarios based on real aircraft structures, and improving experimental data based design guidelines [23].

In line with this VICONOPT has been extended to enable postbuckling analysis [24, 25] of prismatic panels. The method is based on a geometrically non-linear analysis with optional allowance for initial imperfections, and is currently restricted to the VIPASA form of analysis.

After critical buckling has occurred, additional load is carried under a regime in which the stiffness of the panel is reduced by differing amounts owing to the re-distribution of stress among and within the component plates [26]. The ratio of postbuckling to pre-buckling axial stiffness is found by an iterative procedure, which establishes the relationship between the applied longitudinal load and the longitudinal end shortening strain. The stabilizing effect of transverse tension, developed in the central portion of the plate when its longitudinal edges remain straight, has been incorporated into the analysis to improve the overall accuracy.

The method used to perform postbuckling analysis in VICONOPT is a Newton-based iteration scheme [25]. This method uses Newton iterations to give accurate convergence on the critical buckling load and associated mode. At the start of each new cycle, the longitudinal and/or shear strain is incremented by a certain amount. Then, the total applied load, the stress distribution across the structure and the postbuckling mode shape and amplitude can be determined.

A typical example is shown in Fig. 1. A simply supported square panel with four longitudinal stiffeners (Fig. 1(a)) is loaded in longitudinal compression. The local mode shape of initial buckling shown in Fig. 1(b) is sinusoidal and has six half waves along the panel length. The plots of stress against strain in the postbuckling regime based on the assumptions of no mode jumping and therefore a constant but reduced stiffness in the postbuckling region are given in Fig. 1(c) for various locations through the panel, showing that the average postbuckling stiffness of the panel (skin plus stiffeners) is reduced by about one third relative to the prebuckling stiffness. The stiffness in the skin edge portions (location 1), the stiffener flanges (location 2) and stiffener webs (locations 5 and 6) have negligible reduction. However, in the inter-stiffener skin portions (locations 3 and 4)

where there is a large deflection, a large reduction of stiffness has occurred.

In postbuckling optimum design, VICONOPT carries out a postbuckling analysis on the panel before each design cycle. The in-plane stiffness of each plate is then adjusted by using an effective stiffness, which is obtained from the postbuckling results, e.g. Fig. 1(c). The overall longitudinal strain at the design load is predicted by using the average postbuckling stiffness calculated. Then, for each plate load/strain curves are plotted up to this level of strain, so that the effective stiffness of each plate

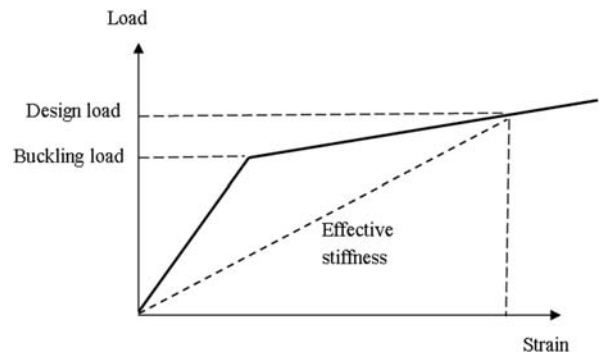


Fig. 2 Calculation of effective stiffness for a post-buckled plate

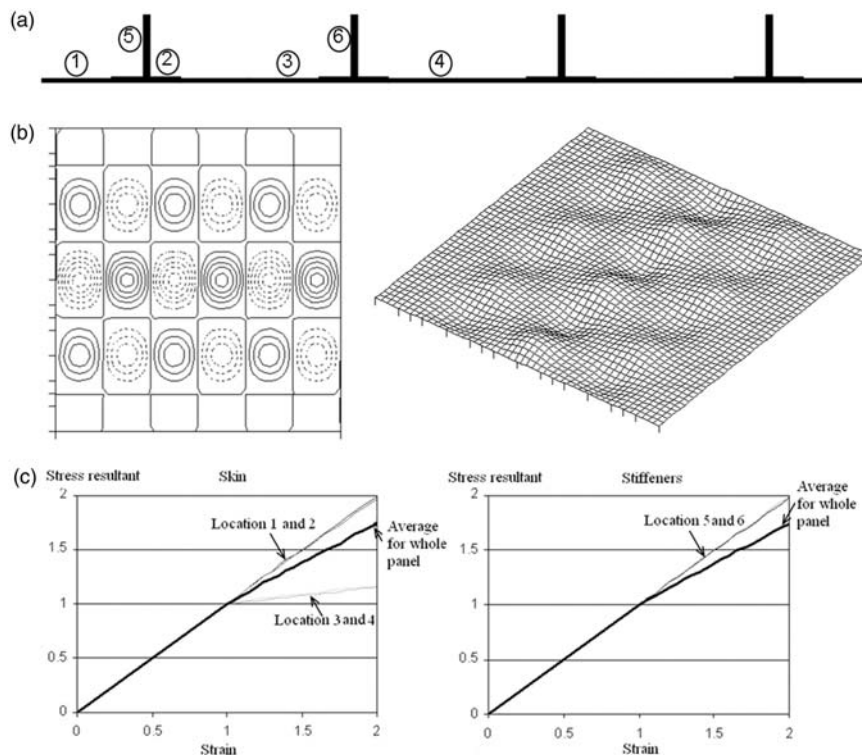


Fig. 1 Postbuckling of a stiffened panel. (a) Panel cross-section. (b) Contour and isometric plots of buckling mode. (c) Normalized axial stress-strain plots at various locations in the skin and stiffeners

can be found by calculating the secant stiffness as shown in Fig. 2.

### 3 VICONOPT MLO

VICONOPT MLO [27] is a Visual C++ program providing a multilevel optimization framework as an interface between VICONOPT and the finite element software MSC/NASTRAN [28] (Fig. 3). Finite element models are created by MSC/PATRAN [29] and a static analysis is performed by MSC/NASTRAN, at an overall or *system* level. VICONOPT MLO then uses the resultant MSC/NASTRAN data (i.e. geometry, material properties, stress distributions, etc.) together with design variables and appropriate bounds defined by the user, to create VICONOPT input files for each of the structure's constituent panels (i.e. at *panel* level). VICONOPT analyses and optimizes each of the panels by minimizing the mass subject to initial buckling constraints. Updated finite element model data, including ply thicknesses, is calculated and returned to MSC/NASTRAN by VICONOPT MLO. Further finite element analysis of the whole structure is carried out with the updated geometry to determine the new stress distributions in each panel. Each panel is now re-optimized. The process is repeated until a convergence criterion specified by the user based on the

overall mass of the structure is met. The dashed portion of Fig. 3 illustrates this part of the multilevel optimization framework which will be referred to as the design cycle.

### 4 MULTILEVEL POSTBUCKLING OPTIMIZATION

The developments to VICONOPT MLO described in this paper allow individual panels to buckle before the design load is reached [30]. These panels continue to carry load with differing levels of effective (i.e. secant) stiffness [25]. VICONOPT MLO creates new MSC/NASTRAN data files based on this effective stiffness data and iterates to converge on an appropriate load re-distribution. Once obtained, this load distribution is used as a starting point in the optimization of the constituent panels as before. As illustrated in Fig. 2, the secant stiffness represents the effective stiffness of each plate at the design load, and so captures the load re-distribution at the load level required in the optimization.

The developments form the new software VICONOPT MLOP, and are illustrated by the solid portion of Fig. 3. Prior to each panel level optimization step, a VICONOPT postbuckling analysis is performed on each panel to determine the postbuckling

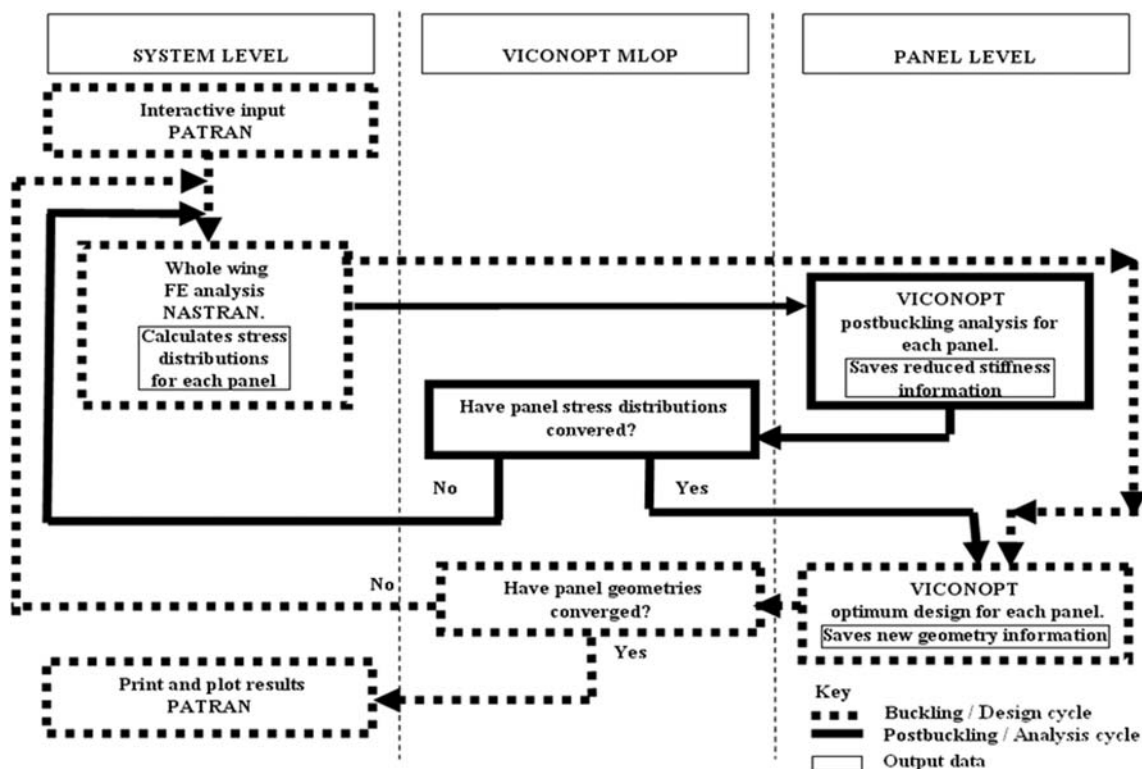


Fig. 3 Multi-level postbuckling framework

stress distribution and the reduced stiffness of each of its component plates. These values will be assumed during the optimization, but it is important to note that they also affect the load-carrying capacity of the postbuckled panel relative to the other panels. It is therefore necessary to repeat the sequence of MSC/NASTRAN system level static analysis until the stress distributions have converged. Panel optimizations then proceed as before, whereby VICONOPT calculates and returns the updated ply thicknesses for each panel to MSC/NASTRAN by VICONOPT MLOP. Then, further finite element analysis of the whole structure is carried out to determine the new stress distributions in each panel. The whole process is repeated until a mass convergence criterion is met. This part of the optimization process, starting with the NASTRAN results and following the solid line, is referred to as the analysis cycle.

## 5 COMPUTATIONAL CONSIDERATIONS

### Mass convergence

As in many optimization problems, one of the biggest challenges in aircraft wing design is convergence, which may take many cycles owing to the large number of design variables. Two different mass convergence checks have been implemented in VICONOPT MLOP, a total mass convergence check and an individual mass convergence check.

The initial total mass of the wing is  $M_0$ . In any design cycle  $i$ , the total mass of the wing is  $M_i$ , and the mass of panel  $j$  is  $m_{j,i}$ .

For the total mass convergence check, the mass will be considered as converged, if

$$\left| \frac{M_i - M_{i-1}}{M_0} \right| \leq \eta \quad (1)$$

where  $\eta$  is the convergence criterion.

For the individual mass convergence check, the initial mass of panel  $j$  will be recorded as  $m_{j,0}$ . The mass of the wing will be considered as converged, only if the mass of each single panel meets the criterion

$$\left| \frac{m_{j,i} - m_{j,i-1}}{m_{j,0}} \right| \leq \eta \quad (2)$$

The number of design cycles performed is strongly affected by the convergence criterion  $\eta$ . In VICONOPT MLOP,  $\eta$  is either defined by the user or a default value 0.01 is used. For the case study described below, the convergence criterion  $\eta$  takes the default value 0.01.

### Load convergence

For each analysis cycle in a design cycle after the first one, the VICONOPT postbuckling analysis is followed by a load convergence check.

For panel  $j$  in analysis cycle  $k$ , suppose the load in a particular panel is  $p_{j,k}^*$ . The largest initial panel load within the current design cycle will be recorded as  $p_{j,0}^*$ . The load in the whole model will be considered as converged, only if the load in each single panel meets the criterion

$$\left| \frac{p_{j,k}^* - p_{j,k-1}^*}{p_{j,0}^*} \right| \leq \eta \quad (3)$$

where the convergence criterion  $\eta$  here is the same as used for the mass convergence check.

In a multilevel postbuckling optimization problem, each panel may take more than one type of loading, e.g. axial load, bending moment, shear load, etc. Each of these will have their own largest initial panel load  $p_{j,0}^*$ . The load of the panel will be considered as converged, only if each component of load (e.g. axial, shear, bending) in this panel meets the criterion.

Once the load changes between two subsequent analysis cycles satisfy the convergence criterion, the postbuckling analysis process for the current design cycle is complete.

### Convergence acceleration

In order to increase efficiency and reduce computational cost, a load convergence acceleration method was used for each component of the load during each analysis cycle.

Suppose the load in a particular panel is  $p$ . In any analysis cycle  $k$  the starting load is  $p_{k-1}^*$  and the predicted load is  $p_k$ . The expected converged result is  $\bar{p}$ . Assume

$$(\bar{p} - p_{k-1}^*) = \alpha(p_k - p_{k-1}^*) \quad (4)$$

where  $\alpha$  is a correction ratio between the predicted step and the required step. It is assumed that  $\alpha$  will take the same value in the next cycle, so that

$$(\bar{p} - p_k^*) = \alpha(p_{k+1} - p_k^*) \quad (5)$$

Solving for  $\alpha$

$$\alpha = \frac{p_k^* - p_{k-1}^*}{p_k + p_k^* - p_{k-1}^* - p_{k+1}} \quad (6)$$

In order to avoid numerical difficulties, if  $\alpha$  is less than 0.01 it is adjusted to 0.01; if  $\alpha$  is greater than 2 it is adjusted to 2. Then the prediction  $p_{k+1}$  is replaced by  $p_{k+1}^*$ , given by

$$p_{k+1}^* = p_k^* + \alpha(p_{k+1} - p_k^*) \tag{7}$$

This acceleration can only be used after two analysis cycles of each design cycle, because the calculation of  $\alpha$  requires two previous results.

**Plates with negative stiffness**

During a postbuckling analysis, some panels contain plates which experience tension, owing to large out-of-plane deflection. These plates will have negative reduced stiffness ratios  $\gamma_x$  as shown in Fig. 4, which are not recognized by MSC/NASTRAN.

In these cases, the value of design loading  $p_{designx}$  for each plate  $x$  is assumed to comprise a

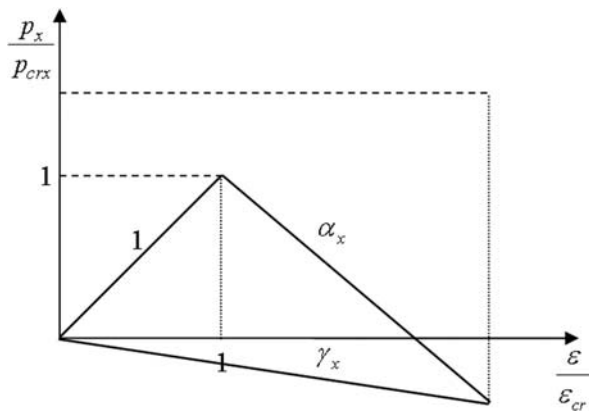


**Fig. 4** Load against end shortening for a plate with negative stiffness ratio

compressive element plus a tensile one as shown in Fig. 5, which is expressed by the formula

$$p_{designx} = p_{comp} + p_{tenx} \tag{8}$$

where  $p_{comp}$  is the assumed compressive load and  $p_{tenx}$  is the assumed tensile load.

Theoretically, an extra pre-buckling stiffness  $\delta^*$  is first applied to all plates to ensure they are under compression as shown in Fig. 6, i.e. point Q replaces point R after postbuckling.

Therefore, in Fig. 6,  $\overline{OP}$  denotes the prebuckling path,  $\overline{PQ}$  denotes the postbuckling path, and  $\overline{QR}$  denotes the necessary adjustment under tensile loading, which is made separately. This gives

$$\frac{p_{comp}}{p_{crx}} = \frac{\gamma_x}{\beta\gamma} + \delta^* \geq 0 \tag{9}$$

and theoretically always has

$$\frac{p_{designx}}{p_{crx}} = \frac{\gamma_x}{\beta\gamma} \tag{10}$$

In order to meet the condition of equation (9) for all plates, the most negative reduced stiffness ratio  $\gamma^* = \min_x \gamma_x$  for the whole wing is used to select  $\delta^*$ , giving

$$\delta^* = -\frac{\gamma^*}{\beta\gamma} \quad (\geq 0) \tag{11}$$

The effective non-negative reduced stiffness ratios  $\gamma_{comp}$  for each plate is then given by

$$\gamma_{comp} = \frac{\frac{p_{comp}}{p_{crx}}}{\frac{\epsilon}{\epsilon_{cr}} + \delta^*} = \frac{\frac{\gamma_x}{\beta\gamma} + \left(\frac{-\gamma^*}{\beta\gamma}\right)}{\frac{1}{\beta\gamma} + \left(\frac{-\gamma^*}{\beta\gamma}\right)} = \frac{\gamma_x - \gamma^*}{1 - \gamma^*} \tag{12}$$

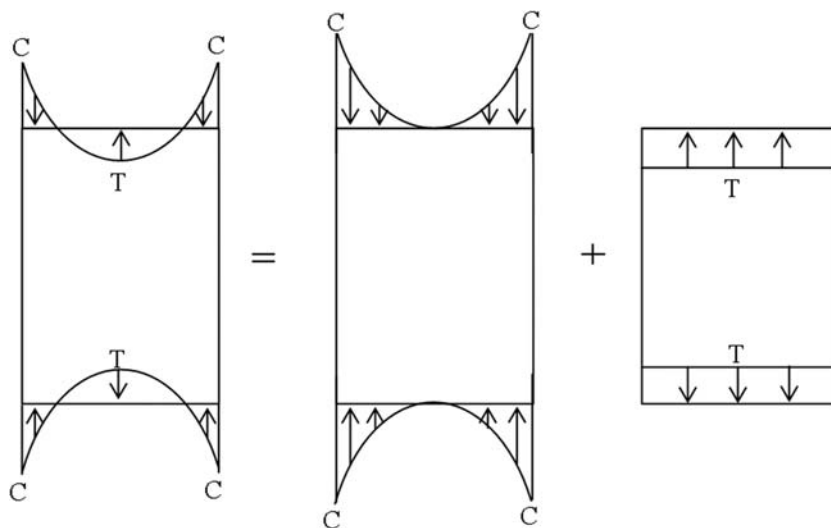


**Fig. 5** Schematic load distributions across a panel

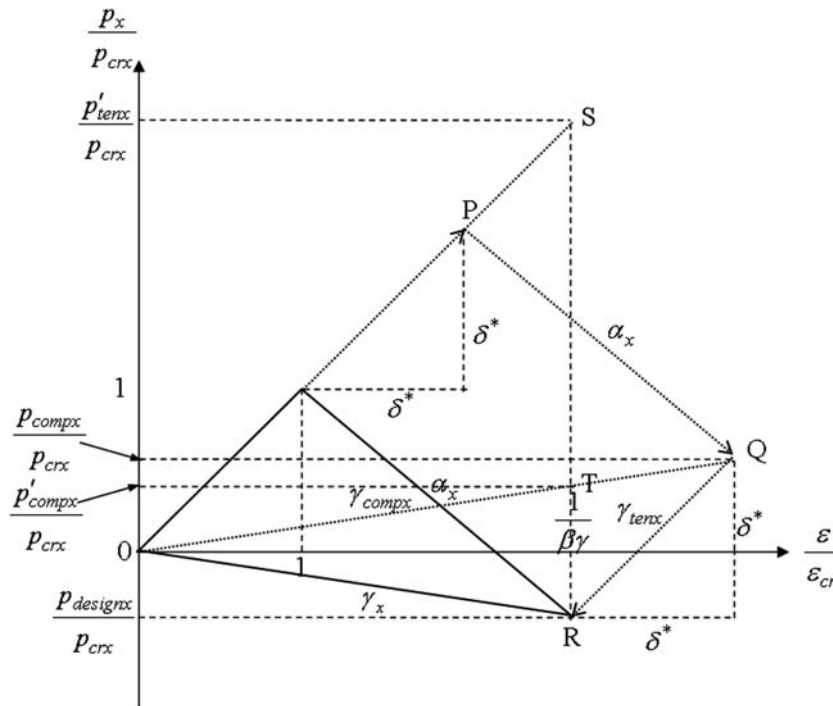


Fig. 6 Theoretical calculation for a plate with negative stiffness ratio

Substituting equation (11) into equation (9) gives

$$\frac{p_{comp}}{p_{crx}} = \frac{\gamma_x}{\beta\gamma} - \frac{\gamma^*}{\beta\gamma} \quad (13)$$

which using equation (10), gives

$$p_{comp} = p_{designx} \left( 1 - \frac{\gamma^*}{\gamma_x} \right) \quad (14)$$

When superposing the assumed tension, the effective stiffness ratio used is

$$\gamma_{tenx} = 1 \quad (15)$$

The assumed tension  $p_{tenx}$  is applied, in order to remove the extra stiffnesses, resulting in

$$\frac{p_{tenx}}{p_{crx}} = -\delta^* = \frac{\gamma^*}{\beta\gamma} \quad (16)$$

which using equation (10), gives

$$p_{tenx} = p_{designx} \left( \frac{\gamma^*}{\gamma_x} \right) \quad (17)$$

MSC/NASTRAN is called twice to find the true design load  $p_{designx}$  for VICONOPT, once for compression and once for tension.

The first time MSC/NASTRAN is called, the most negative reduced stiffness ratio for the whole wing  $\gamma^* = \min_x \gamma_x$  is determined and the MSC/NASTRAN input file is created using the effective non-negative reduced stiffness ratios  $\gamma_{comp}$  for each plate, given by

equation (12). The applied compressive load  $p'_{comp}$  calculated by MSC/NASTRAN is given by the point T in Fig. 6, which corresponds to a normalized strain of  $\frac{1}{\beta\gamma}$  and reduced stiffness ratio  $\gamma_{comp}$ . This is expressed by

$$\frac{p'_{comp}}{p_{crx}} = \frac{\gamma_{comp}}{\beta\gamma} = \frac{\gamma_x - \gamma^*}{1 - \gamma^*} \quad (18)$$

Substituting equation (10) into equation (18) gives

$$p'_{comp} = p_{designx} \frac{\gamma_x - \gamma^*}{(1 - \gamma^*)\gamma_x} \quad (19)$$

Then, from equations (14) and (19), it can be seen that

$$p_{comp} = p'_{comp}(1 - \gamma^*) \quad (20)$$

i.e. the requirement that the compressive loads  $p'_{comp}$  calculated by MSC/NASTRAN are all multiplied by the positive factor  $(1 - \gamma^*)$ .

MSC/NASTRAN is now called for a second time, with effective reduced stiffness ratios for each plate given by  $\gamma_{tenx} = 1$ , giving an applied tensile load  $p_{tenx}$  as shown by the point S in Fig. 6, which also corresponds to a normalized strain of  $\frac{1}{\beta\gamma}$ . This is expressed by

$$\frac{p'_{tenx}}{p_{crx}} = \frac{\gamma_{tenx}}{\beta\gamma} = \frac{1}{\beta\gamma} \quad (21)$$

Substituting equation (10) into equation (21) gives



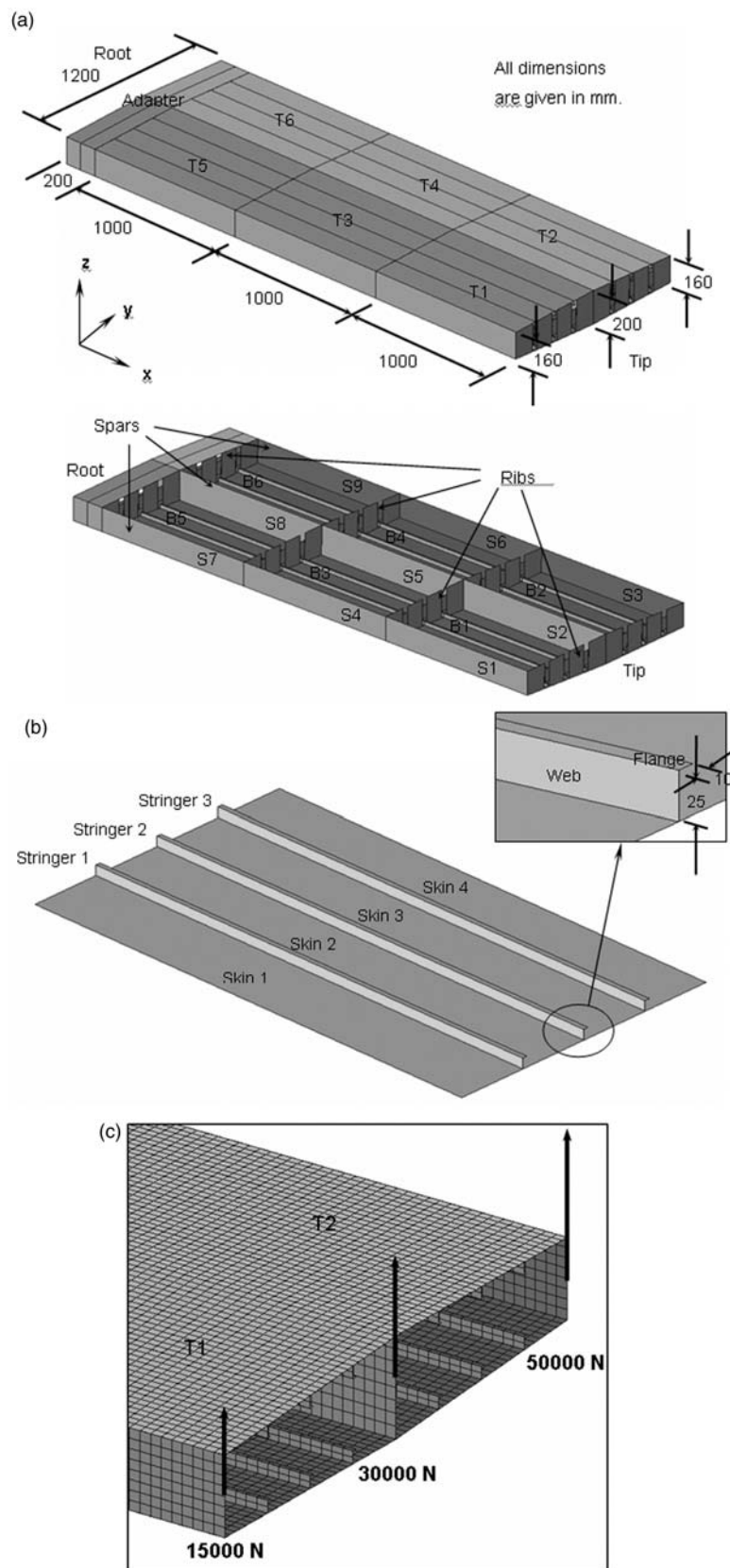


**Fig. 7** (a) Wing structure showing skin panels, spars and ribs; (b) typical skin panel, showing skin plates and stringers; (c) load case:twist

**Table 1** Material properties of high strength carbon-epoxy (GARTEUR [14–16])

High-strength carbon-epoxy		
Longitudinal Young's modulus	$E_1 (N/mm^2)$	140 000
Transverse Young's modulus	$E_2 (N/mm^2)$	10 000
In-plane shear modulus	$G_{12} (N/mm^2)$	5000
Major Poisson's ratio	$\nu$	0.3
Ultimate longitudinal tensile strength	$\max .\sigma_{1t} (N/mm^2)$	1500
Ultimate longitudinal compressive strength	$\max .\sigma_{1c} (N/mm^2)$	1200
Ultimate transverse tensile strength	$\max .\sigma_{2t} (N/mm^2)$	50
Ultimate transverse compressive strength	$\max .\sigma_{2c} (N/mm^2)$	250
Ultimate in-plane shear strength	$\max .\tau_{12} (N/mm^2)$	70
Density	$\rho (g/mm^3)$	0.0016

**Table 2** Initial ply thicknesses, upper and lower bounds (all in mm)

		Initial design	Lower bound	Upper bound
T1, T2, B1, B2 (Tip)				
Skin	45° and –45° plies	0.250	0.125	1.500
	90° plies	0.500	0.125	1.500
	0° plies	0.500	0.125	1.500
Web	45° and –45° plies	0.125	0.125	1.500
	90° plies	0.250	0.125	1.500
	0° plies	1.500	0.125	1.500
Flange	45° and –45° plies	0.125	0.125	1.500
	90° plies	0.250	0.125	1.500
	0° plies	1.500	0.125	1.500
T3, T4, B3, B4 (Middle)				
Skin	45° and –45° plies	0.375	0.125	1.500
	90° plies	0.625	0.125	1.500
	0° plies	1.000	0.125	1.500
Web	45° and –45° plies	0.250	0.125	1.500
	90° plies	1.250	0.125	1.500
	0° plies	2.000	0.125	2.000
Flange	45° and –45° plies	0.250	0.125	1.500
	90° plies	1.250	0.125	1.500
	0° plies	2.000	0.125	2.000
T5, T6, B5, B6 (Root)				
Skin	45° and –45° plies	0.500	0.125	1.500
	90° plies	0.750	0.125	1.500
	0° plies	1.500	0.125	1.500
Web	45° and –45° plies	0.375	0.125	1.500
	90° plies	2.250	0.125	2.250
	0° plies	2.500	0.125	2.500
Flange	45° and –45° plies	0.375	0.125	1.500
	90° plies	2.250	0.125	2.250
	0° plies	2.500	0.125	2.500
Spars S1-S9				
	45° and –45° plies	0.375	0.188	0.563
	90° plies	1.500	0.750	2.250
	0° plies	4.000	2.000	6.000

$$p'_{tenx} = \frac{p_{designx}}{\gamma_x} \quad (22)$$

Then, from equations (11) and (22), it can be seen that

$$p_{tenx} = p'_{tenx}\gamma^* \quad (23)$$

i.e. the compressive loads  $p'_{tenx}$  calculated by MSC/ NASTRAN are all scaled by the negative factor  $\gamma^*$  to give tensile loads.

Finally, the load calculations from equations (20) and (23) are substituted into equation (8) to determine the real applied design load  $p_{designx}$  for VICONOPT. VICONOPT MLOP carries out this

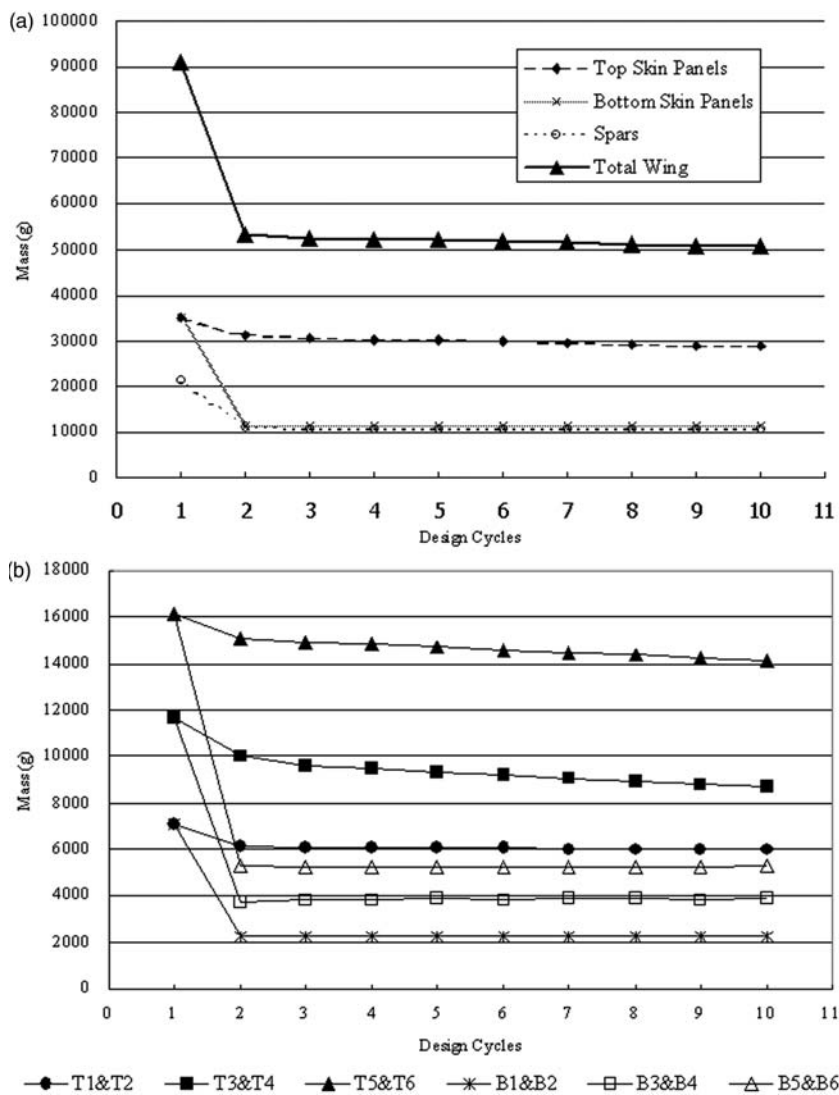


**Fig. 8** Mass changes during the multilevel optimization process (a) total mass changes, (b) mass changes in adjacent panels

**Table 3** Changes of mass in designs obtained by VICONOPT MLO. and VICONOPT MLOP. Percentage changes are relative to the initial design

		Top skin	Bottom skin	Spars	Total
Initial design		34935 g	34935 g	21216 g	91086 g
Final design	Previous solution VICONOPT MLO	55081 g (+57.67%)	10308 g (-70.49%)	21216 g ( $\pm 0\%$ )	86605 g (-4.92%)
	New solution VICONOPT MLOP	28796 g (-17.57%)	11416 g (-67.32%)	10612 g (-49.98%)	50825 g (-44.20%)

whole process automatically if any negative stiffnesses are found.

In practical terms, MSC/NASTRAN not only has difficulty in considering negative stiffnesses, but also zero stiffnesses. In order to avoid zero stiffnesses, values of  $\delta^*$  are always taken to be slightly larger than those calculated from equation (8).

## 6 AIRCRAFT WING DESIGN

A case study based on recommendations made by GARTEUR [14–16] was conducted into the optimization of the schematic composite aircraft wing shown in Fig. 7(a), in order to demonstrate the capabilities of VICONOPT MLOP.

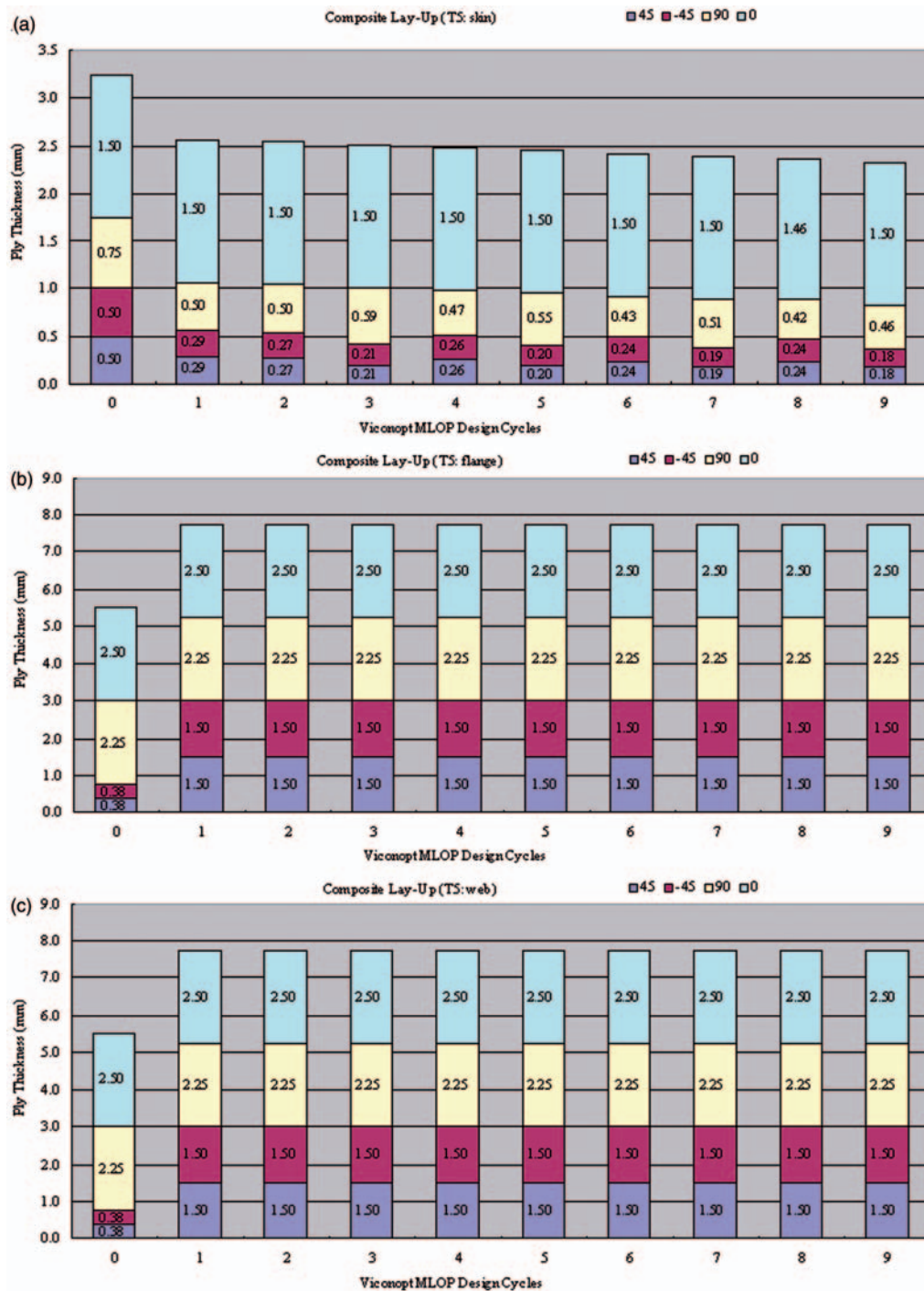


Fig. 9 Changes of ply thicknesses in panel T5, (a) skin, (b) flange and (c) web

The wing contains 12 skin panels, six at the top and six at the bottom, three spars and four ribs (Fig. 7(a)). The objective was to optimize the ply thicknesses in each of the skin and spar panels. No attempt was made to optimize the ribs, which were included in the model to provide simply supported edge conditions for the skin.

Three L-shaped stringers are connected to each skin panel using rigid displacement constraints (i.e. degrees of freedom involving displacement at coincident points in the skin and stringer are constrained to be the same). These stringers provided increased longitudinal stiffness and increase the local buckling capacity of the skin. This configuration results in a

total of ten plates to be defined: four skin plates, three webs and three flanges (Fig. 7(b)). Individual property cards were specified in the MSC/NASTRAN model for each of the component plates, in order to account for the variation of reduced postbuckling stiffness, and also allowing the user to define separate design variables for each plate. A uniform mesh consisting of 29 280 quadrilateral elements (QUAD4) was generated for the overall wing, which resulted in a model with 126 860 degrees of freedom. To model realistic boundary conditions, the root of the wing was attached to a steel adapter, which was fully clamped at its free end. The optimization covered panels T1–T6 on the top skin, panels B1–B6 on the bottom skin and panels S1–S9 on the three spars. The ribs were assumed to be of fixed dimensions and sufficient to provide simple support to the skin panels. Figure 7(b) shows details of the skin/stringer configuration for each of the 12 skin panels.

The loading of Fig. 7(c) was considered, which twists the wing about its longitudinal axis. This is the most testing of the two load cases taken from the GARTEUR recommendations. It primarily generates axial loads and bending moments in the panels. The relatively small shear and transverse loads were ignored during the postbuckling analysis. During the optimization, buckling was permitted at a minimum of 50 per cent of the design load.

High-strength carbon-epoxy was used as the material for the individual laminae of all component plates. Table 1 summarizes the properties in the principal material directions, together with the material density and the ultimate material strengths, which were used as allowable limits in the optimization. The onset of damage below these limits was not considered in the present study.

In the initial design, each plate has a symmetric balanced lay-up ( $-45^\circ/45^\circ/90^\circ/0^\circ/90^\circ/45^\circ/-45^\circ$ ) with different thicknesses for skin, web and flange plates and spars. The initial ply thicknesses and the design variables in the VICONOPT models for each panel and spar are shown in Table 2.

## 7 NUMERICAL RESULTS

An initial static finite element analysis was carried out for the overall wing by MSC/NASTRAN, Then VICONOPT models were generated for the individual skin panels and spars using VICONOPT MLOP. A total 135 design variables were specified for the ply thicknesses of their component plates.

VICONOPT MLOP carried out a total of ten multi-level optimization cycles, before the strictest convergence criterion for the mass of each panel was met. Figure 8(a) shows the mass changes during the

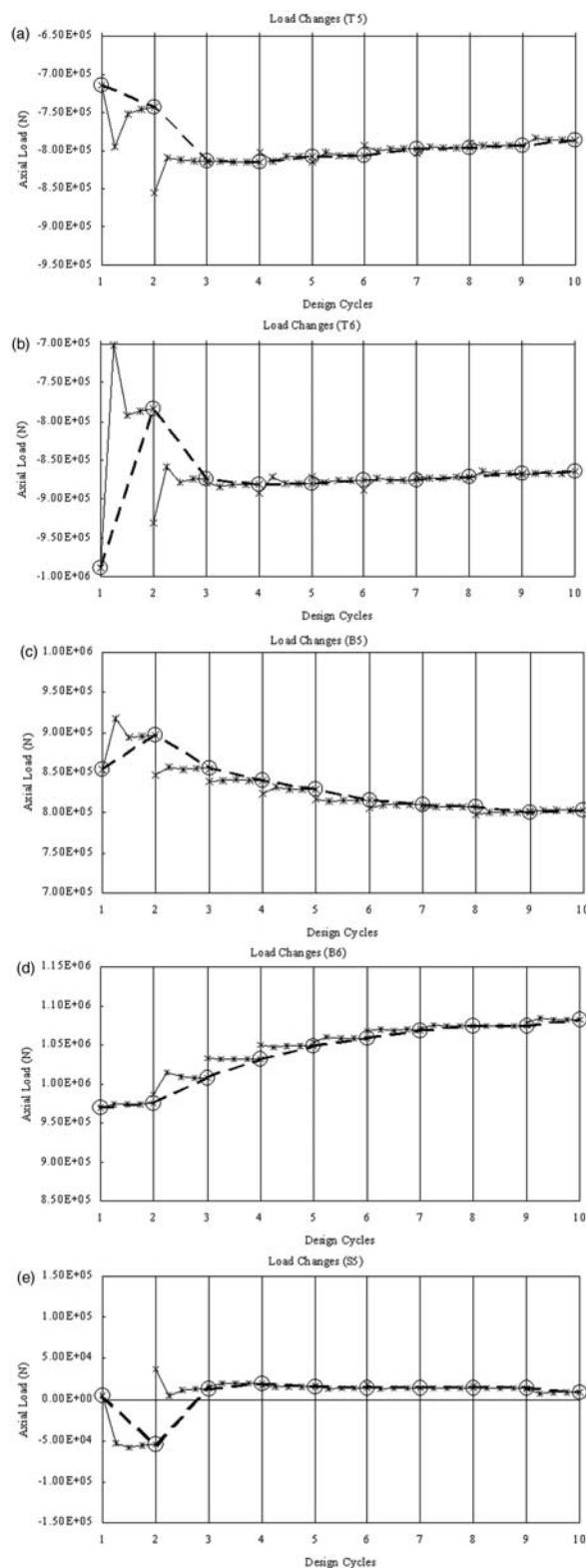


**Fig. 10** Load changes during the multilevel optimization process: top skin panels (a) T5, (b) T6; bottom skin panels (c) B5, (d) B6; spar panel (e) S5

multilevel optimization process. It can be seen that the total mass of the wing converged well on a value of approximately 50 kg, which represented a total saving of 44 per cent over the initial design. All the panels experienced a decrease in mass. But the mass of the bottom skin panels reduced much more significantly than the top panels, owing to them being in tension. Figure 8(b) shows mass changes for the individual pairs of panels on the top and bottom skin panels. As expected, the root panels which are required to carry higher loads (panels T5, T6, B5, and B6) had more material assigned to them than the tip panels

(panels T1, T2, B1, and B2). The mass of the spars reduced by 50 per cent over the initial design, maintaining approximately the same percentage of wing mass and therefore avoiding attracting an artificially high percentage of the load.

Comparison of these VICONOPT MLOP results with those obtained using the previous code VICONOPT MLO [31], shows significant advantages in terms of mass savings, as shown in Table 3. The top skin panels previously increased in mass, but decreased in mass in VICONOPT MLOP when post-buckling was allowed. Changes in mass in the bottom

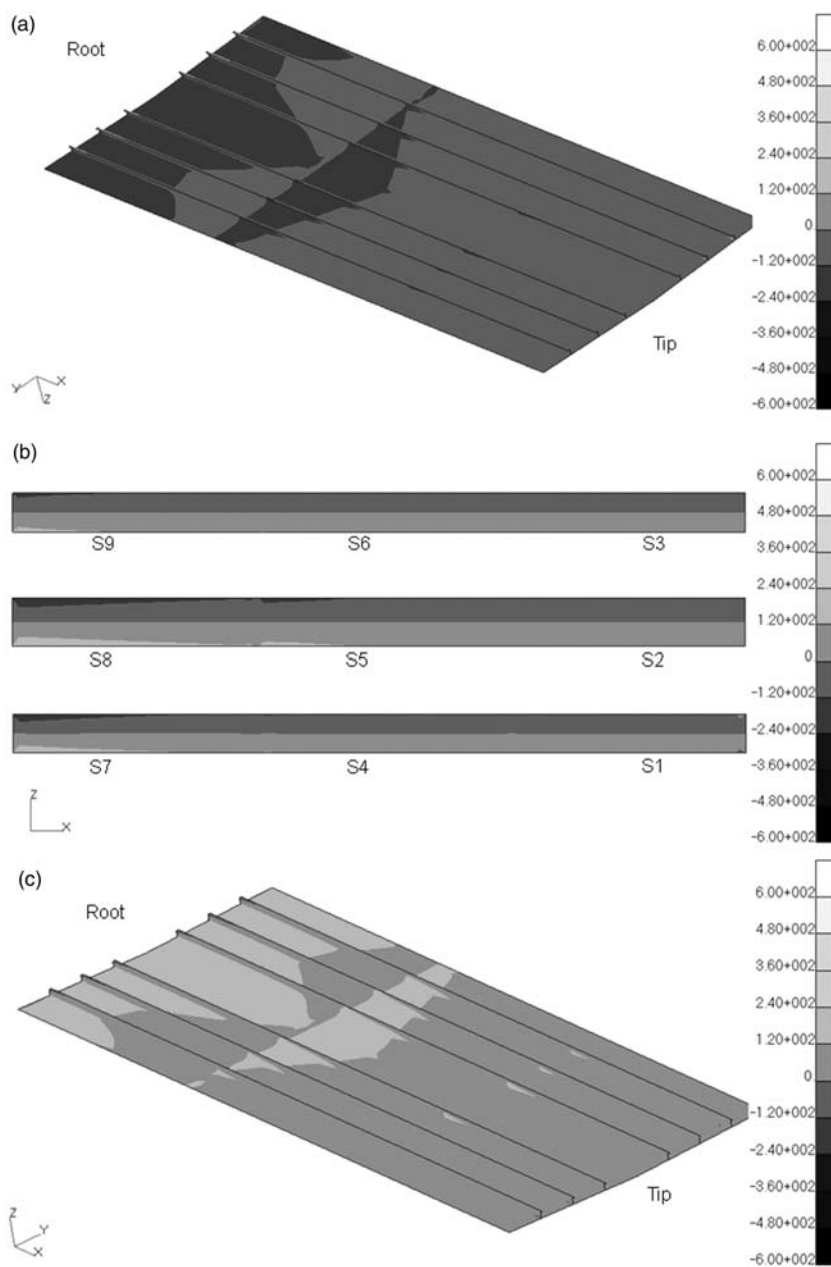


**Fig. 11** Longitudinal stress contours for the initial designs, (a) top skin (b) spars (c) bottom skin ( $N/mm^2$ )

skin panels were similar in the two solutions; since their design was limited by stress constraints and not by buckling. Significant weight reduction has been achieved in the spars, which remain unbuckled, since these were not designed in the previous solution, but have been considered in the new one.

The total mass of the wing showed very good convergence after three design cycles (Fig. 8(a)); the optimization carried on however, owing to mass/load changes in individual panels. The number of design cycles could be reduced by applying a looser

convergence criterion  $\eta$  instead of the 1 per cent used during the optimization. For example, if  $\eta$  is set to 0.03, the number of design cycles can be reduced to approximately seven, and if  $\eta$  is 0.05 this number can be reduced to four.

During optimization, the bottom skin panels did not buckle because they carried large tension loads together with negligible shear loads. In these cases, the VICONOPT MLOP design is governed by strength constraints rather than buckling. In the final design, the ply thicknesses of tension panels B1 and B2

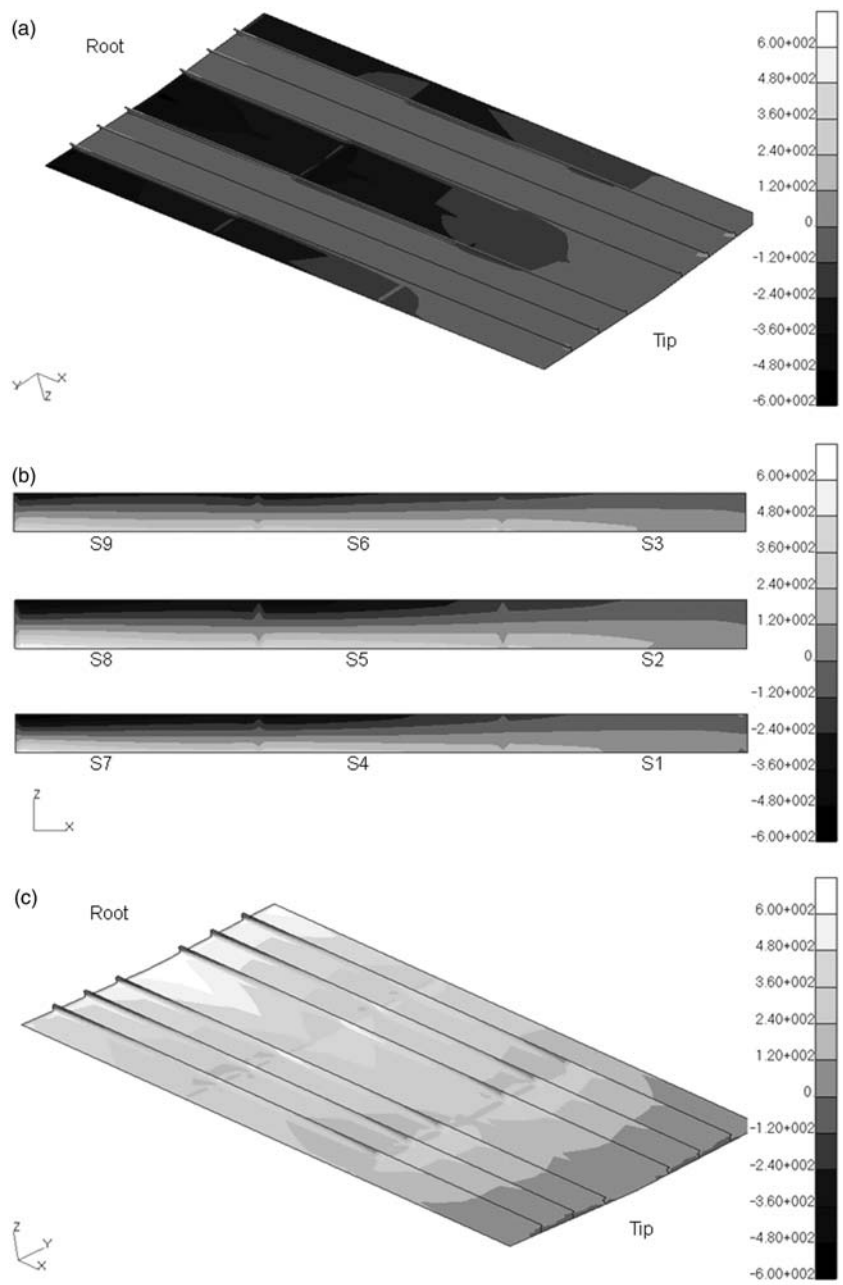


**Fig. 12** Longitudinal stress contours for the final designs, (a) top skin (b) spars and (c) bottom skin (N/mm<sup>2</sup>)

reached their lower bounds, but panels B3–B6 did not, because the tension near the root of wing was too large to avoid the stress constraints.

Figure 9 shows the ply thickness changes for panel T5. In this compression panel, almost all of the  $0^\circ$  layers, which take most of the loading, reach their upper bounds. All the flange thicknesses are increased to give enough stiffness to carry the loading. The ply thicknesses in the webs are increased because additional stiffness is required after the flanges have reached their upper bounds. The thicknesses of the  $\pm 45^\circ$  layers are increased to carry shear loads. Details of the ply thickness changes for the remaining thicknesses can be found in Qu [32].

Figure 10 shows the load changes in top skin panels T5 and T6, bottom skin panels B5 and B6 and spar panel S5. The converged load in each design cycle is indicated by a circle. By applying the convergence acceleration method of section 5.2, the panel loads in each design cycle converged well within four analysis cycles. During each design cycle, owing to the changes in geometry and postbuckling stiffness, the loads changed significantly.

Contours of longitudinal stress for the initial and final designs are shown in Figs 11 and 12 respectively. In the initial design, the skin panels are under approximately uniform and symmetrical loading with slight increases from the tip to the root (Figs 11(a) and (c)) and the stress in the spar panels varies linearly through the wing depth (Fig. 11(b)). After the optimization, since the overall ply thicknesses of each panel were reduced and became different from those in adjacent panels, the stress distributions became asymmetric and varied significantly through the length and depth of the wing (Fig. 12). Figure 12(a) shows that the stress in the top skin panels is concentrated around the spars which provide effective simple support to the skin.

## 8 CONCLUSIONS

VICONOPT MLO was developed as a Windows based interface, linking the well-known finite element package MSC/NASTRAN and the specialist panel design code VICONOPT, in order to perform efficient optimization of complex structures by using the much faster exact strip method to design individual panels while the more complicated overall wing structure is analysed using finite element analysis. The development reported here enables substantial additional savings in terms of mass and therefore cost to be achieved by incorporating postbuckling effects.

A case study of a whole aircraft wing is presented in this paper. This has enabled a more detailed insight into the multilevel optimization and postbuckling

behaviour of such complicated structures to be gained. The results of the study show the total mass of the whole wing reduced by 44 per cent throughout the optimization, and skin panels reduced by approximately 42 per cent. This compares to the results from the previous version of VICONOPT MLO [22], with a further 36 per cent of total mass saved.

The multilevel optimization carried out proved to be very efficient and displayed good convergence. Although the finite element model at system level was very large and a lot of data had to be transferred between the different levels, owing to the efficiency of VICONOPT MLO, the multilevel optimization process required only 10–15 min to complete an analysis cycle on a Core™ 2 Duo, 2GHz, 1.96GB RAM, and of the overall solution time, less than 10 per cent was spent in VICONOPT.

Further work is required to evaluate the method for alternative load cases, more complicated structures, e.g. damaged panels and non-rectangular panels, and also to allow for practical manufacturing requirements.

## FUNDING

This research received no specific grant from any funding agency in the public, commercial, or not-for-profit sectors.

© Authors 2011

## REFERENCES

- Altair Engineering.** *Engineering design optimisation course lecture notes*, 2000 (Altair Engineering Ltd, Alderton, Northamptonshire, UK).
- Courant, R.** Variational methods for the solution of problems of equilibrium and vibrations. *Bull. Am. Math. Soc.*, 1943, **49**(1), 1–23.
- Carroll, C. W.** The created response surface technique for optimizing nonlinear restrained systems. *Ops Res.*, 1961, **9**, 169–184.
- Fiacco, A. V. and McCormick, G. P.** *Nonlinear programming, sequential unconstrained minimization techniques*, 1968 (Wiley, New York).
- Vanderplaats, G. N.** *Numerical Optimisation techniques for engineering design*, 1984 (McGraw-Hill, New York).
- Williams, F. W., Kennedy, D., Butler, R., and Anderson, M. S.** VICONOPT: program for exact vibration and buckling analysis or design of prismatic plate assemblies. *AIAA J.*, 1991, **29**, 1927–1928.
- Kennedy, D., Fischer, M., and Featherston, C. A.** Recent developments in exact strip analysis and optimum design of aerospace structures. *Proc. IMech, Part C: J. Mechanical Engineering Science*, 2007, **221**(4), 399–413.



- 8 **Wittrick, W. H.** and **Williams, F. W.** A general algorithm for computing natural frequencies of elastic structures. *Q. J. Mechanics Appl. Math.*, 1971, **24**(3), 263–284.
- 9 **Wittrick, W. H.** and **Williams, F. W.** An algorithm for computing critical buckling loads of elastic structures. *J. Struct. Mechanics*, 1973, **1**(4), 497–518.
- 10 **Wittrick, W. H.** and **Williams, F. W.** Buckling and vibration of anisotropic or isotropic plate assemblies under composite plate assemblies. *Int. J. Mech. Sci.*, 1974, **16**(4), 209–239.
- 11 **Almroth, B. O.** and **Brogan, F. A.** The STAGS computer code. NASA CR-2950 1978.
- 12 **Butler, R.** and **Williams, F. W.** Optimum design using VICONOPT, a buckling and strength constraint program for prismatic assemblies of anisotropic plate. *Comput. Struct.*, 1992, **43**(4), 699–708.
- 13 **Anderson, M. S., Williams, F. W.,** and **Wright, C. J.** Buckling and vibration of any prismatic assembly of shear and compression loaded anisotropic plates with an arbitrary supporting structure. *Int. J. Mech. Sci.*, 1983, **25**(8), 585–596.
- 14 **GARTEUR** System level structural optimisation: A compendium of European aerospace programs. Final report of the GARTEUR Action Group on Structural Optimisation SM(AG13) [open literature]. Volume 1 of 3, GARTEUR TP078, 1997a (DERA, Farnborough, UK).
- 15 **GARTEUR** A compendium of European software facilities for stiffened plate design and multilevel optimisation. Final report of the GARTEUR Action Group on Structural Optimisation SM(AG13) [open literature]. Volume 2 of 3, GARTEUR TP079, 1997b (DERA, Farnborough, UK).
- 16 **GARTEUR** Assessment of benchmark problems on stiffened panel design and multilevel optimisation. Final report of the GARTEUR Action Group on Structural Optimisation SM(AG13) [limited literature]. Volume 2 of 3, GARTEUR TP080, 1997c (DERA, Farnborough, UK).
- 17 **Bisagni, C.** and **Lanzi, L.** Post-buckling optimisation of composite stiffened panels using neural networks. *Composite Structs.*, 2002, **58**, 237–247.
- 18 **Kalnins, K., Jekabsons, G.,** and **Rikards, R.** Metamodels for optimisation of post-buckling responses in full-scale composite structures. In Proceedings of 8th World Congress on Structural and multidisciplinary optimisation, Lisbon, Portugal, 2009.
- 19 **Fares, M. E., Youssif, Y. G.,** and **Elshoraky, A. E.** Non-linear design and control optimisation of composite laminated plates with buckling and postbuckling objectives. *Int. J. Non-Linear Mechanics*, 2006, **41**, 807–824.
- 20 **Lanzi, L.** and **Giavotto, V.** Post-buckling optimisation of composite stiffened panels computations and experiments. *Composite Struct.*, 2006, **73**(2), 208–220.
- 21 **van Houten, M. H.** and **Zdunek, A.** Post-buckling and collapse analysis, final technical report. GARTEUR SM(AG25) TP-149, 2004.
- 22 **Zimmermann, R.** and **Rolfes, R.** POSICOSS-improved postbuckling simulation for design of fibre composite stiffened fuselage structure. *Composite Struct.*, 2006, **73**(2), 171–174.
- 23 **Degenhardt, R., Rolfes, R. R., Zimmermann, R.,** and **Rohwer, K.** COCOMAT-improved material exploitation of composite airframe structures by accurate simulation of postbuckling and collapse. *Composite Struct.*, 2006, **73**(2), 175–178.
- 24 **Powell, S. M., Williams, F. W., Askar, A. S.,** and **Kennedy, D.** Local postbuckling analysis for perfect and imperfect longitudinally compressed plates and panels. In Proceedings of the 39th AIAA/ASME/ASCE/AHS/ASC Conference on *Structures, structural dynamics and materials conference*, Long Beach, CA, 1998, pp. 595–603.
- 25 **Anderson, M. S.** and **Kennedy, D.** Postbuckling of composite stiffened panels using exact strip analysis with Newton iteration. In Proceedings of the 49th AIAA/ASME/ASCE/AHS/ASC Conference on *Structures, structural, dynamics and materials*, 2008, Paper AIAA-2008-2184, pp. 1–8.
- 26 **Anderson, M. S.** Design of panels having postbuckling strength. In Proceedings of the 38th AIAA/ASME/ASCE/AHS/ASC Conference on *Structures, structural, dynamics and materials*, 1997, pp. 2407–2413.
- 27 **Fischer, M., Kennedy, D.,** and **Featherston, C. A.** Multilevel optimisation of aerospace and lightweight structures. In Proceeding of the 23rd International Congress on *Aeronautical sciences*, 2002, pp. 344.1–344.9.
- 28 **MSC/Software.** *MSC/NASTRAN version 70.7*, 1999 (MSC, Los Angeles).
- 29 **MSC/Software.** *MSC/PATRAN Version 9.0*, 1999 (MSC, Los Angeles).
- 30 **Qu, S., Kennedy, D.,** and **Featherston, C. A.** Multilevel postbuckling design of aerospace structures. In Proceedings of 8th World Congress on Computational mechanics and 5th European Congress on computational methods in applied sciences and engineering, 2008. ISBN 978-84-96736-55-9.
- 31 **Fischer, M., Kennedy, D.,** and **Featherston, C. A.** Multilevel optimisation of a composite aircraft wing using VICONOPT MLO. In Proceeding of the 9th AIAA/ISSMO Symposium on *Multidisciplinary analysis and optimization*, 2002, AIAA-2002-5511. ISBN 1-56347-535-9.
- 32 **Qu, S.** *Multilevel optimisation of aerospace and lightweight structures incorporating postbuckling effects*. PhD Thesis, Cardiff University, 2011.